Understanding the Role of *Eed* Deletion in Medulloblastoma

Mehal Churiwal

Department of Psychology and Neuroscience, University of North Carolina College of Arts and Sciences, Chapel Hill, NC USA

ABSTRACT

Medulloblastoma, the most common malignant pediatric brain cancer, is uniquely sensitive to DNA damage-inducing therapies, with conventional treatment resulting in an 80% 5-year survival rate. Researching the apoptotic pathways that make treatment effective in some tumors and how those pathways contribute to resistance in others may identify therapies that reduce the need for toxic radiation and chemotherapy. In cerebellar development, physiologic Sonic Hedgehog (SHH) signaling drives proliferation of cerebellar granule neuron progenitors (CGNPs). Similarly, pathologic SHH hyperactivation drives proliferation in SHH-subgroup medulloblastoma, which makes up 30% of medulloblastoma cases. SHH signaling upregulates target genes in part by preventing H3K27 trimethylation marks via the JMJD3/KDM6B demethylase complex. In differentiated cerebellar neurons, where SHH signaling is low, the polycomb repressive complex 2 (PRC2) silences SHH target genes by trimethylating H3K27 residues in regulatory regions.

Our data show that blocking the PRC2 through genetic deletion has varying effects in different contexts. When the PRC2-component *Eed* is deleted in SHH-subtype medulloblastomas that form in mice engineered for SHH hyperactivation, the tumors show initially slower growth compared to tumors in *Eed*-intact controls; however, the mice have significantly poorer survival. Therefore, this study aims to understand the mechanisms of initially reduced tumor growth and ultimately more rapid tumor progression. Our recent single cell gene expression analysis showed that *Eed* deletion in CGNPs induced genes involved in muscle cell differentiation, including myogenin and troponin. We will characterize *Eed*-deleted medulloblastoma using fluorescence-activated cell sorting (FACS) as well as immunohistochemistry (IHC). The first aim of this study is to elucidate how cell cycle dynamics are altered in *Eed*-deleted medulloblastomas. The second aim of the study tests whether *Eed* deletion alters the levels of cell cycle markers, cell death, and aberrant expression of muscular proteins in SHH-driven medulloblastoma. Our cell cycle studies show that *Eed* deletion slows tumor growth in early development, but the tumor later develops EED independence, resulting in more rapid progression and decreased survival. Additionally, our data show that *Eed* deletion alters the expression of proteins related to proliferation, differentiation, apoptosis, and muscle development.

INTRODUCTION

Medulloblastoma

The regulation of apoptosis is vital for both normal brain growth and the response of brain tumors to therapy.[1] Excessive apoptosis of cerebellar granule neuron progenitors (CGNPs) can result in cerebellar hypoplasia,[2,3] and failure to induce apoptosis can lead to medulloblastoma formation.[4] Medulloblastoma, the most common malignant pediatric brain cancer, occurs in a region of the brain called the cerebellum, which is responsible for motor learning, maintaining a sense of body position and posture, retaining balance and equilibrium, and other fine movement coordination (**Figure 1**). This form of cancer is uniquely sensitive to DNA damage-inducing treatments such as radiation (**Figure 2**). Conventional treatment plans include a combination of radiation, chemotherapy, and surgical resection, which results in a 5-year survival rate of 80%.[5] Although 80% of patients are sensitive to radiation and chemotherapy, treatment still fails 20% of patients. Moreover, the treatment is highly toxic, causing long-lasting impacts on young patients who are still developing. These impacts include endocrine abnormalities, growth impairments, hearing loss, and cognitive decline.[6,7,8] Thus, it's important to research the apoptotic pathways that make treatment effective in some patients but not in others. Understanding how apoptosis is regulated during cerebellar development and medulloblastoma in mice can provide valuable information about possible new therapeutic targets for medulloblastoma treatment in humans.[4,5,9] Gaining a better understanding of these mechanisms may lead to the development of treatment options that efficiently disrupt normal functioning to induce apoptosis in tumors; intervention at the molecular level can help reduce the need for radiation and chemotherapy, thus lowering the toxicity of treatment for medulloblastoma.

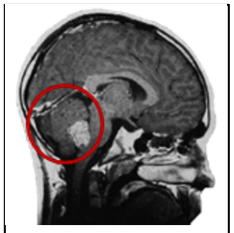

Figure 1: Medulloblastoma tumors occur in the cerebellum region of the brain.
Reference: Huang, *Medscape*, 2017

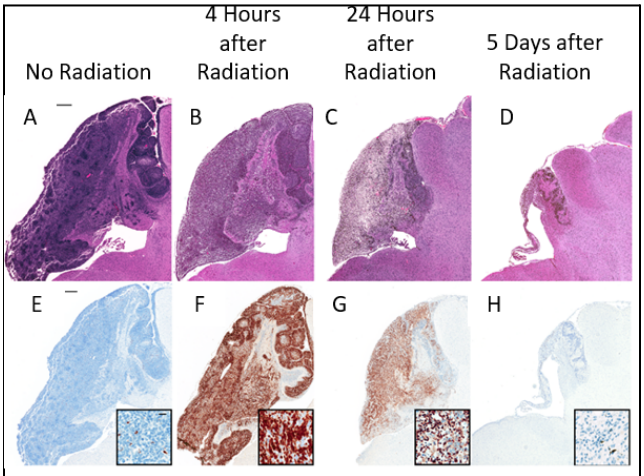

Figure 2: Mouse model for medulloblastoma that recapitulates the radiation sensitivity seen in human patients to radiation. Images (A)-(D) use H&E staining to show the deteriorating anatomy of the tumor long after radiation. Images (E)-(H) use cC3 staining to show the large increase in apoptosis caused by radiation due to which the tumor decreases in size.
Reference: Crowther, *Cancer Res.*, 2016

SHH Signaling

In early cerebellar development, Sonic Hedgehog (SHH) signaling drives the proliferation of cerebellar granule neuron progenitors (CGNPs). This proliferation is needed to form the cerebellar granule neurons (CGNs), the largest neuronal population in the human brain.[10] The proliferating CGNPs are localized in the external

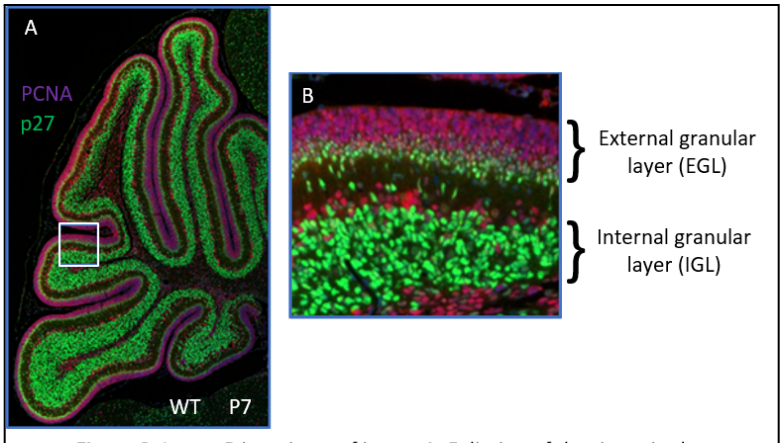

Figure 3: Image B is an inset of image A. Foliation of the tissue in the cerebellum, showing the external granular layer (EGL) stained in purple with PCNA and the internal granular layer (IGL) stained in green with p27. The cerebellar granule neuron progenitors (CGNPs) are primarily found in the EGL of the cerebellum.

granular layer (EGL) of the cerebellum; as these proliferating CGNPs differentiate into CGNs, they migrate towards the internal granular layer (IGL) of the cerebellum (**Figure 3**). However, if SHH is hyperactivated, it can promote the over-proliferation of CGNPs, which can eventually lead to the development of SHH-subgroup medulloblastoma.[11] This is the most common type of medulloblastoma, with approximately 30% of medulloblastoma cases falling within this subgroup.

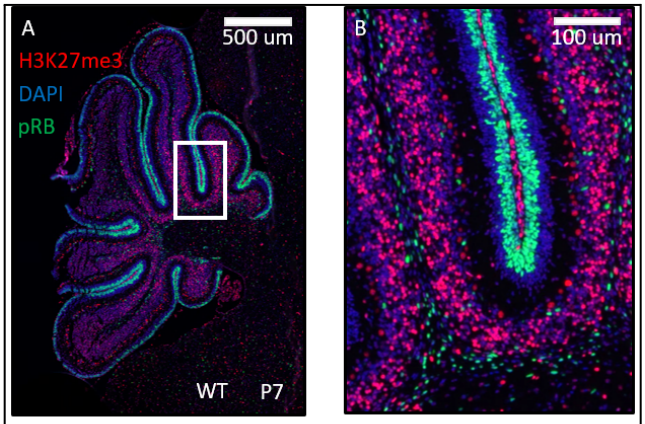

Figure 4: Image (B) is an inset of image (A). The proliferating cells are shown in green using pRB; they are concentrated in the EGL and are less concentrated in the IGL; nuclei are labeled in blue using DAPI. The H3K27 trimethylation, shown in red, is in very low concentrations in the proliferating EGL cells but increases dramatically in the differentiating IGL cells.

SHH signaling has been shown to regulate the activity of the polycomb repressive complex 2 (PRC2), a chromatin modifying complex, in CGNPs.[12] When SHH signaling is not active, the PRC2 complex interacts with the regulatory regions of the SHH target genes and trimethylates H3K27 residues in order to repress the expression of those genes. However, when SHH signaling is present, it drives expression of target genes by displacing the PRC2 complex and removing H3K27 trimethylation marks via the JMJD3/KDM6B demethylase complex, which also recruits activating SET1/MLL H3K4 methyltransferases to further enhance the expression of the target genes.[12] Accordingly, proliferating CGNPs localized in the EGL, which would have high levels of SHH, have been shown to have low H3K27 trimethylation levels due to the displacement of the PRC2 complex; on the other hand, differentiating CGNs, which have low levels of SHH, accumulate higher levels of H3K27 trimethylation as the neurons migrate from the EGL to the IGL because of the replacement of the PRC2 complex (**Figure 4**). Due to PRC2's role in regulating proliferation and differentiation of CGNPs, it could play a role in either supporting or resisting the formation of medulloblastoma tumors.[13]

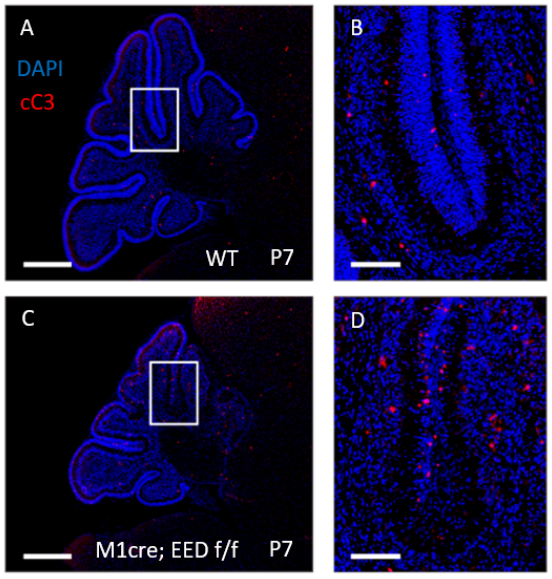

Figure 5: Image (B) is an inset of image A, while image (D) is an inset of image (C). Cerebella tissue harvested at P7, where neuronal cells are stained in blue using DAPI and cC3, shown in red, is a molecular marker for apoptosis. Images A and B are from an EED wt sample, showing low amounts of apoptosis, whereas images C and D are from an EED f/f sample, showing higher amounts of apoptosis.

Eed Deletion

Research from the Gershon lab shows that mitosis-inducing SHH signaling plays a key role in regulating apoptosis in CGNPs and in medulloblastoma,[14] thereby making PRC2 a central target of study. The PRC2 is composed of a number of proteins, two of the key components being EZH2 and EED. EZH2 is the catalytic subunit of PRC2 that trimethylates H3K27 residues. EED supports the role of EZH2 by binding to trimethylated H3K27 residues to enhance the suppression of those genes.[15] Thus, research projects in the Gershon lab focus on understanding the effects of conditionally deleting *Eed* to better interrogate the role of PRC2 in cerebellar development and medulloblastoma.

To study how altering the epigenetic balance of SHH-driven CGNPs affects apoptotic priming, Abigail Cleveland (a PhD candidate in the Gershon lab) conditionally deleted *Eed* in CGNPs

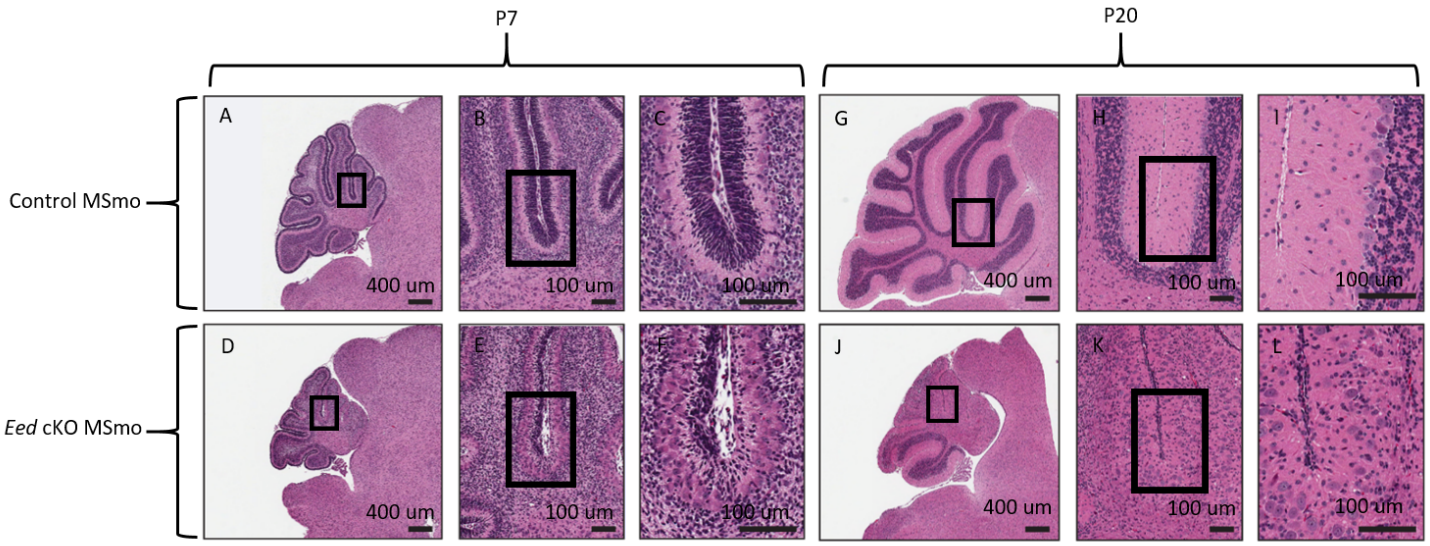

Figure 6: Images (A)-(C) are from a P7 control MSmo sample, whereas images (D)-(F) are from a P7 *Eed* cKO Msmo sample, showing increased cerebellar disorganization and hypoplasia caused by the conditional deletion of *Eed*. Images (G)-(I) are from a P20 control MSmo sample, whereas images (J)-(L) are from a P20 *Eed* cKO Msmo sample, showing cerebellar disorganization and hypoplasia caused by the conditional deletion of *Eed* that is more exaggerated than seen in P7 samples.

of mice. Her findings showed that conditional deletion of *Eed* causes CGNPs to undergo apoptosis (**Figure 5**), disrupting cerebellar growth and leading to cerebellar hypoplasia (**Figure 6**). Additionally, through immunohistochemical studies, Abigail found that *Eed*-deleted cerebella have decreased proliferation (pRB+) at P7, but this proliferation is prolonged into P20 through the presence of the EGL. In wildtype cerebella, by the time mice reach P14, proliferation is completed and the EGL is eliminated. Additionally she saw less differentiated (NeuN+) CGNs, and increased expression of p21, a cell cycle inhibitor. More surprisingly, single cell gene expression analysis showed that *Eed* deletion in CGNPs caused the induction of genes involved in muscle cell differentiation, including myogenin and troponin.

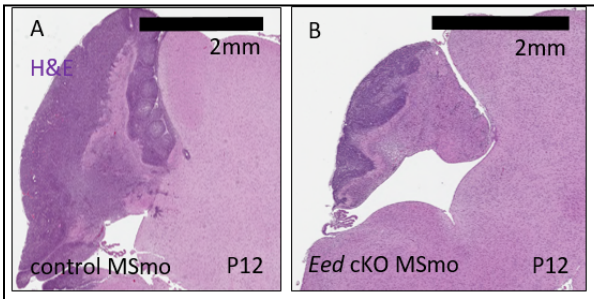

Figure 7: H&E staining in (A) control MSmo tumors and (B) *Eed* cKO MSmo tumors shows drastic changes in the histology of MSmo tumors depending on the presence of *Eed*.

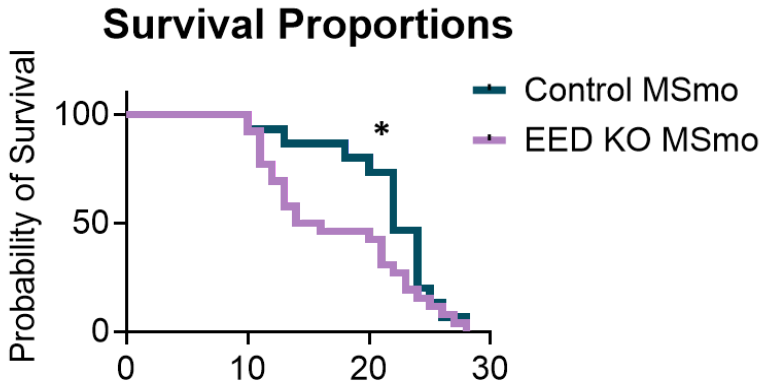

Figure 8: Survival curves for *Eed* cKO MSmo and control MSmo mice. "*" indicates that $p \leq 0.05$; "**" indicates that $p \leq 0.01$; "***" indicates that $p \leq 0.001$.

When *Eed was deleted in SHH medulloblastomas, it resulted in smaller tumors than Eed-intact controls* (**Figure 7**); *however, the mice had significantly poorer survival* (**Figure 8**). Given these perplexing outcomes, this study aims to better characterize the role of *Eed* deletion in medulloblastoma. The first aim of this study is to elucidate how cell cycle dynamics are altered in *Eed*-deleted medulloblastomas. The second aim of the study tests whether *Eed* deletion alters the levels of cell cycle markers,

cell death, and aberrant expression of muscular proteins in SHH-driven medulloblastoma. The successful completion of this project will inform future research regarding the role of EED in medulloblastoma. The hope is that by better understanding the mechanisms through which *Eed* deletion induces spontaneous apoptosis and possibly alters cell cycle dynamics of CGNPs, researchers could use that knowledge to develop more effective therapeutic options to treat medulloblastoma tumors in patients.

METHODS

Breeding

To model SHH-subtype medulloblastoma in mice, we bred *Math1-Cre* mice, which express Cre recombinase in the Math1+ CGNP population, with mice expressing a constitutively-active mutant smoothened allele (SmoM2). The resulting *M1cre; SmoM2 (MSmo)* mice develop SHH medulloblastoma tumors by 14 days old. We also bred the MSmo line with $Eed^{loxP/loxP}$ mice. This generated *Math1-Cre; SmoM2;*$Eed^{loxP/loxP}$ (*Eed* cKO MSmo) mice in which *Eed* is deleted in the CGNP population.

Age Points

Eed cKO MSmo and control MSmo tumors were collected at postnatal day 12 (P12) for immunohistochemical studies. Additionally, to assess how EED deletion impacts the cell cycle dynamics of tumors over the course of time, mice were collected at both P12 and at P18, the age at which approximately 50% of the *Eed* cKO MSmo mice survived.

Gating Definitions for Each Phase	
G0	pRB-
G1	pRB+ / EdU- / 2n DNA
S	pRB+ / EdU+
G2	pRB+ / EdU- / 4n DNA
M	pRB++

Table 1: These are the gating definitions used for each cell cycle phase to develop an appropriate gating workflow.

Fluorescence-Activated Cell Sorting (FACS)

Tumor cells from harvested medulloblastomas were dissociated from 6 *Eed* cKO MSmo and 5 control MSmo mice at P12 as well as from 3 *Eed* cKO MSmo and 4 control MSmo mice at P18. Mice were first injected with EdU 1 hour prior to harvest to label cells in S phase. To determine whether *Eed* cKO MSmo tumors have different cell cycle dynamics, the dissociated cells were stained for cell cycle markers

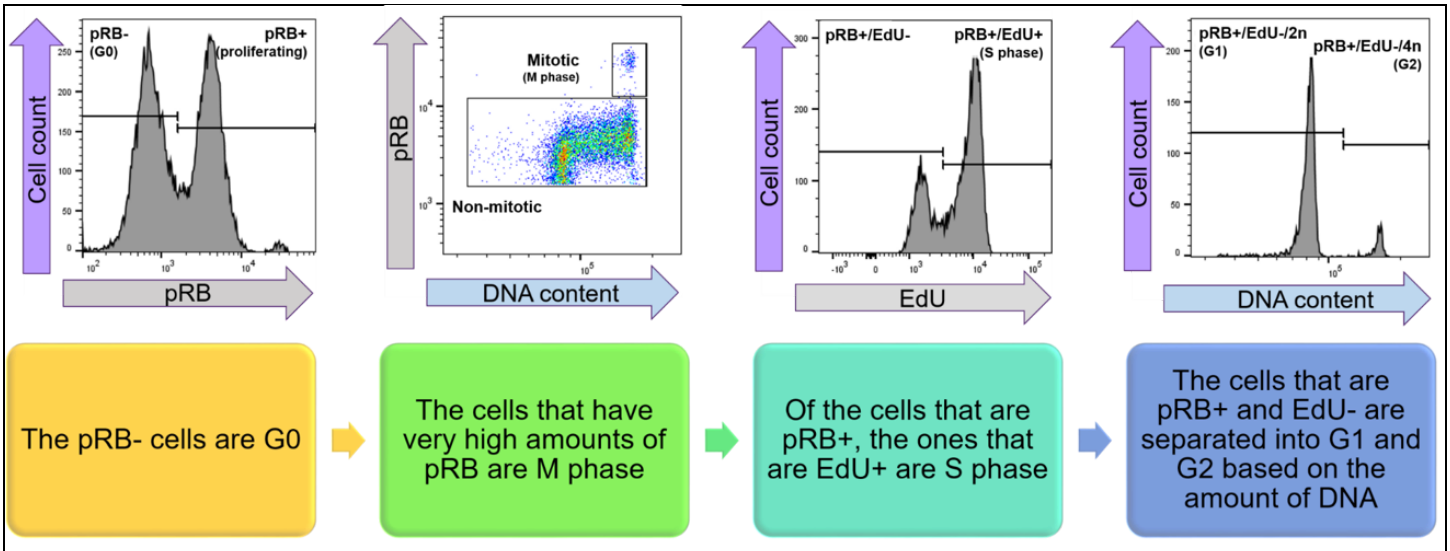

Figure 9: This series demonstrates the gating procedure that was implemented to classify cells using a P18 *Eed* cKO sample as an example.

5-ethynyl-2´-deoxyuridine (EdU), pRB, and FX cycle violet (DNA content marker) before performing fluorescence-activated cell sorting (FACS). The results from FACS were analyzed using FlowJo software (**Table 1**). First, certain gating logistics were applied to remove any unwanted debris and doublets, after which cells in G0 were defined as pRB negative and cells in M phase as highly pRB positive. Of the remaining cells that were positive for pRB, the ones that were also positive for EdU were classified as S phase cells. The remaining cells that were positive for pRB and negative for EdU were divided into G1 and G2 based on their DNA content: cells with 2n DNA were in G1, and cells with 4n were in G2 (**Figure 9**). Once these counts were recorded, the percentage of cells in G0, G1, S, G2, and M phase out of the total number of cells were calculated and also the percentage of cells in G1, S, G2, and M phase out of the total number of pRB positive cells was calculated.

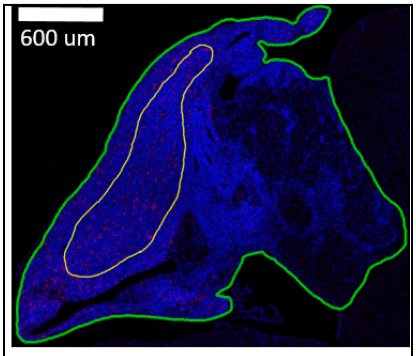

Figure 10: Example of annotations done on a myogenin stain. The green line indicates the whole tumor, whereas the yellow line indicates a hypercellular region of interest.

Immunohistochemistry (IHC)

Tumors were also harvested from *Eed* cKO MSmo mice and *Eed*-intact MSmo controls for immunohistochemistry (IHC). The harvested tumors were then stained with markers for cell cycling, cell death, and muscle proteins, after which the images were annotated to define the whole tumor. For myogenin, a region high in tissue density (region of interest) was also annotated (**Figure 10**). Each of the stains in the images were quantified for the annotated regions.

Statistical Analyses

Data from FACS cell cycle studies were analyzed using two statistical procedures. In order to assess whether proliferation significantly differed both between genotypes (*Eed* cKO MSmo and control MSmo) and ages (P12 and P18), unpaired two-tailed t-tests were performed. However, when comparing the distribution across several cell cycle phases simultaneously, t-tests cannot be used because each of the phases must be analyzed as a single collective vector rather than treating each phase independent of the other phases. Instead, Dirichlet regressions were performed to compare the distribution of proliferating cells in different cell cycle phases (G1, S, G2, and M) between genotypes (*Eed* cKO MSmo and control MSmo) and ages (P12 and P18). All FACS data was analyzed using R x64 4.0.2. To analyze significance in the IHC data, unpaired two-tailed t-tests were conducted between the *Eed* cKO and control MSmo mice. All IHC data was analyzed using GraphPad Prism 9.

RESULTS

Fluorescence Activated Cell-Sorting (FACS)

To understand how EED deletion impacts cell cycle dynamics, the percentage of proliferating cells were measured in *Eed* cKO MSmo and control MSmo samples after which the proliferating cells were gated into more specific cell cycle phases. At P12, there were less proliferating cells in *Eed* cKO MSmo tumors than in MSmo control tumors (**Figure 11A**), but this difference between genotypes was eliminated by the time mice reached P18 (**Figure 11B**). At both age points, the distribution of proliferating cells across the four cell cycle phases were statistically different between the two genotypes; more specifically, there was an increased proportion of proliferating cells in S phase in the *Eed* cKO MSmo mice (**Figure 11C-D**). When doing cross-age

comparisons, there is a significant increase in the number of proliferating cells from P12 to P18 in *Eed* cKO MSmo mice ($p < 0.001$). However, no such statistical difference is seen in control MSmo mice. Similarly, the distribution of proliferating cells across the four cell cycle phases is statistically different at P12 and P18 in *Eed* cKO MSmo mice; specifically, there was a decrease in the proportion of mitotic cells at P18 ($p < 0.05$). However, no statistical difference in the distribution of proliferating cells among cell cycle phases existed in control MSmo mice between P12 and P18.

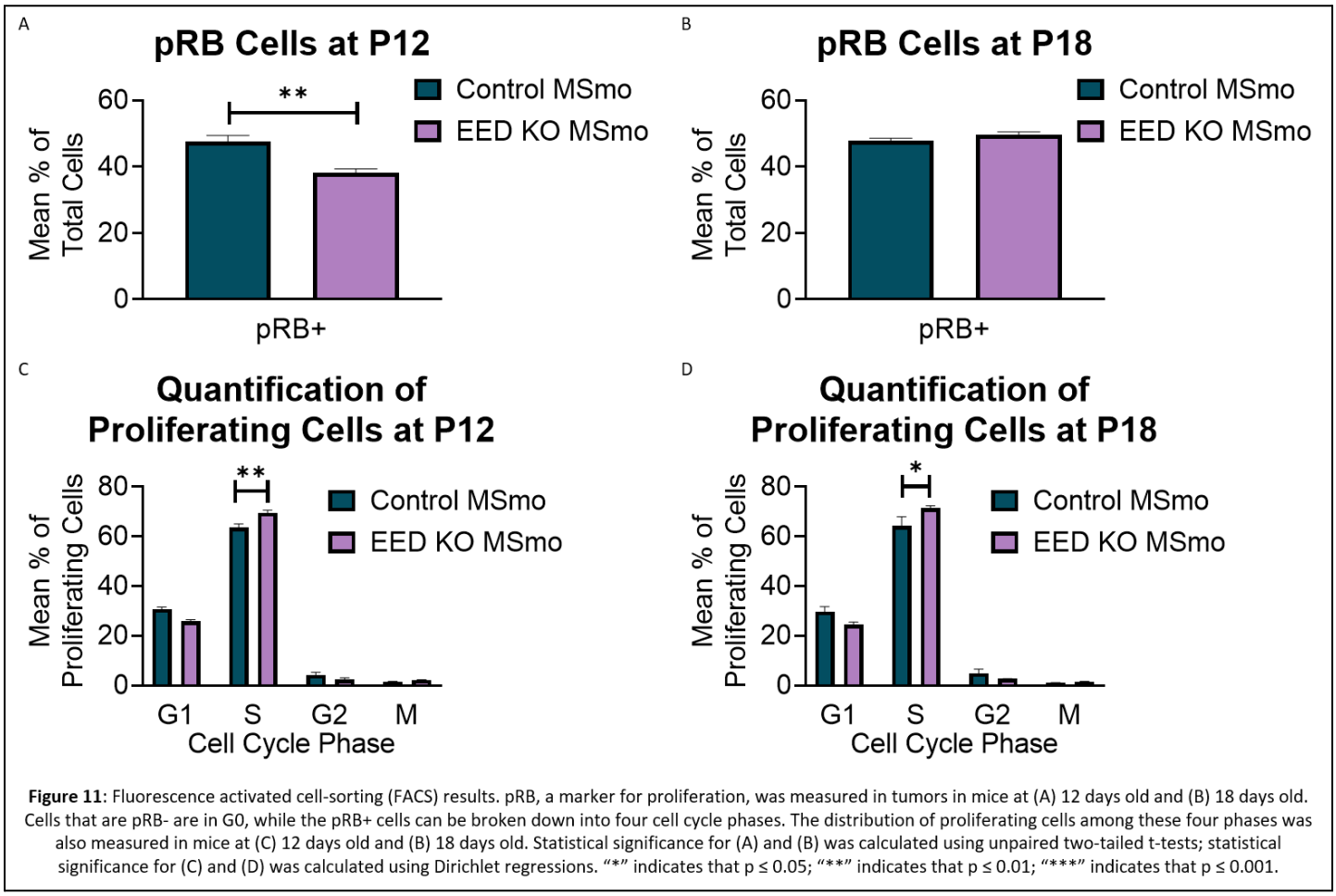

Figure 11: Fluorescence activated cell-sorting (FACS) results. pRB, a marker for proliferation, was measured in tumors in mice at (A) 12 days old and (B) 18 days old. Cells that are pRB- are in G0, while the pRB+ cells can be broken down into four cell cycle phases. The distribution of proliferating cells among these four phases was also measured in mice at (C) 12 days old and (B) 18 days old. Statistical significance for (A) and (B) was calculated using unpaired two-tailed t-tests; statistical significance for (C) and (D) was calculated using Dirichlet regressions. "*" indicates that $p \leq 0.05$; "**" indicates that $p \leq 0.01$; "***" indicates that $p \leq 0.001$.

Immunohistochemistry (IHC)

IHC analysis was used to determine whether EED alters cell cycling and differentiating markers in MSmo tumors. *Eed* deletion significantly reduced both proliferation (pRB+; **Figure 12A**) and neural differentiation (NeuN+; **Figure 12B**) in *Eed* cKO MSmo tumors compared to control MSmo tumors, but we found no significant differences when comparing expressions of p21 (**Figure 12C**) or Cdkn1C (**Figure 12D**).

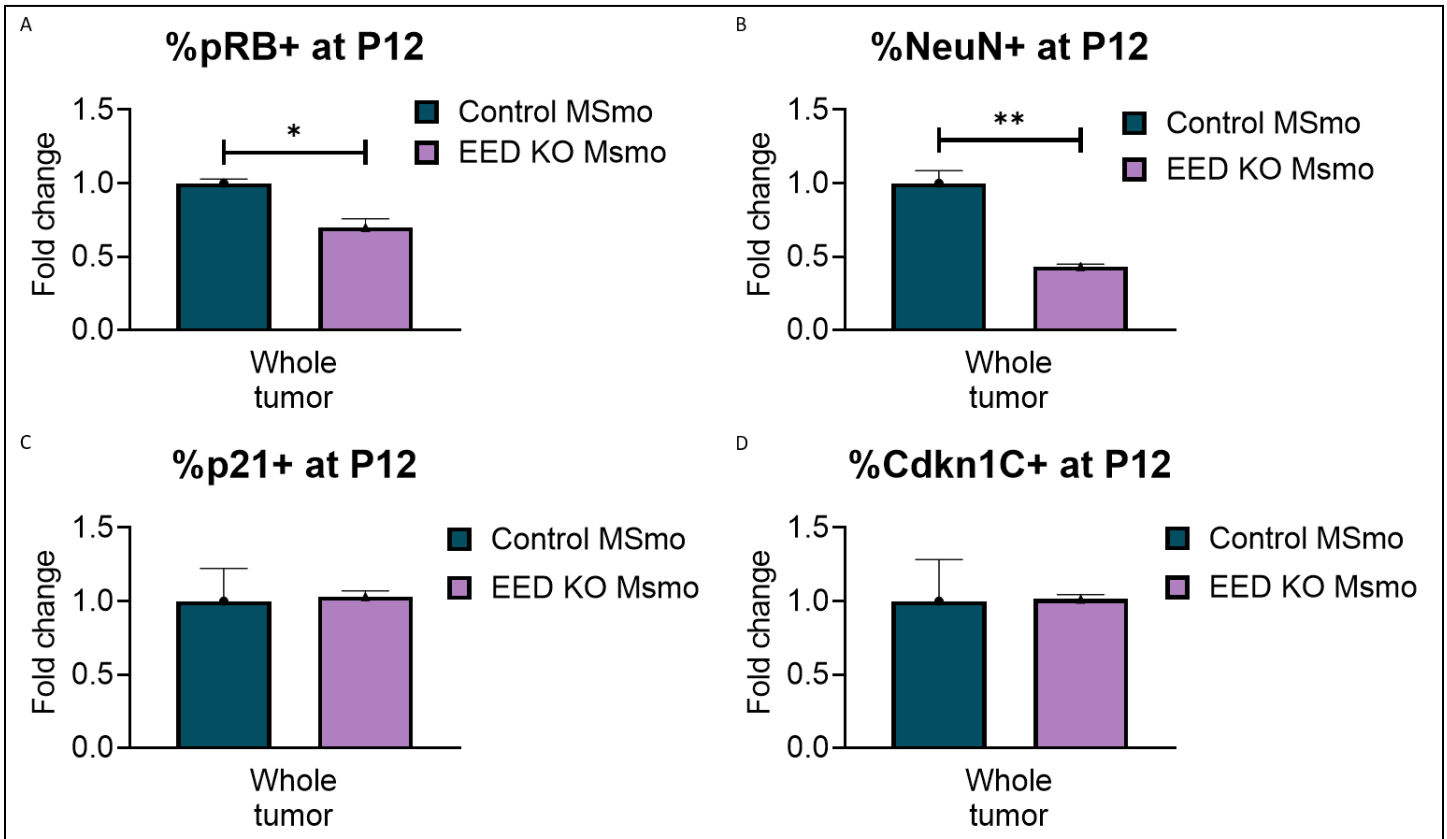

Figure 12: Immunohistochemistry (IHC) results for cell cycling markers. (A) pRB is a marker for proliferation (B) NeuN is a marker for differentiation (C) p21 is a cell cycling inhibiting CDK (D) Cdkn1C is a tumor suppression protein. Statistical significance was calculated using unpaired two-tailed t-tests. "*" indicates that $p \leq 0.05$; "**" indicates that $p \leq 0.01$; "***" indicates that $p \leq 0.001$.

Compared to control MSmo tumors, *Eed* cKO MSmo had significantly less independent expression of apoptosis (**Figure 13A**) and DNA damage (**Figure 13B**) as well as less co-expression of the two (**Figure 13C**).

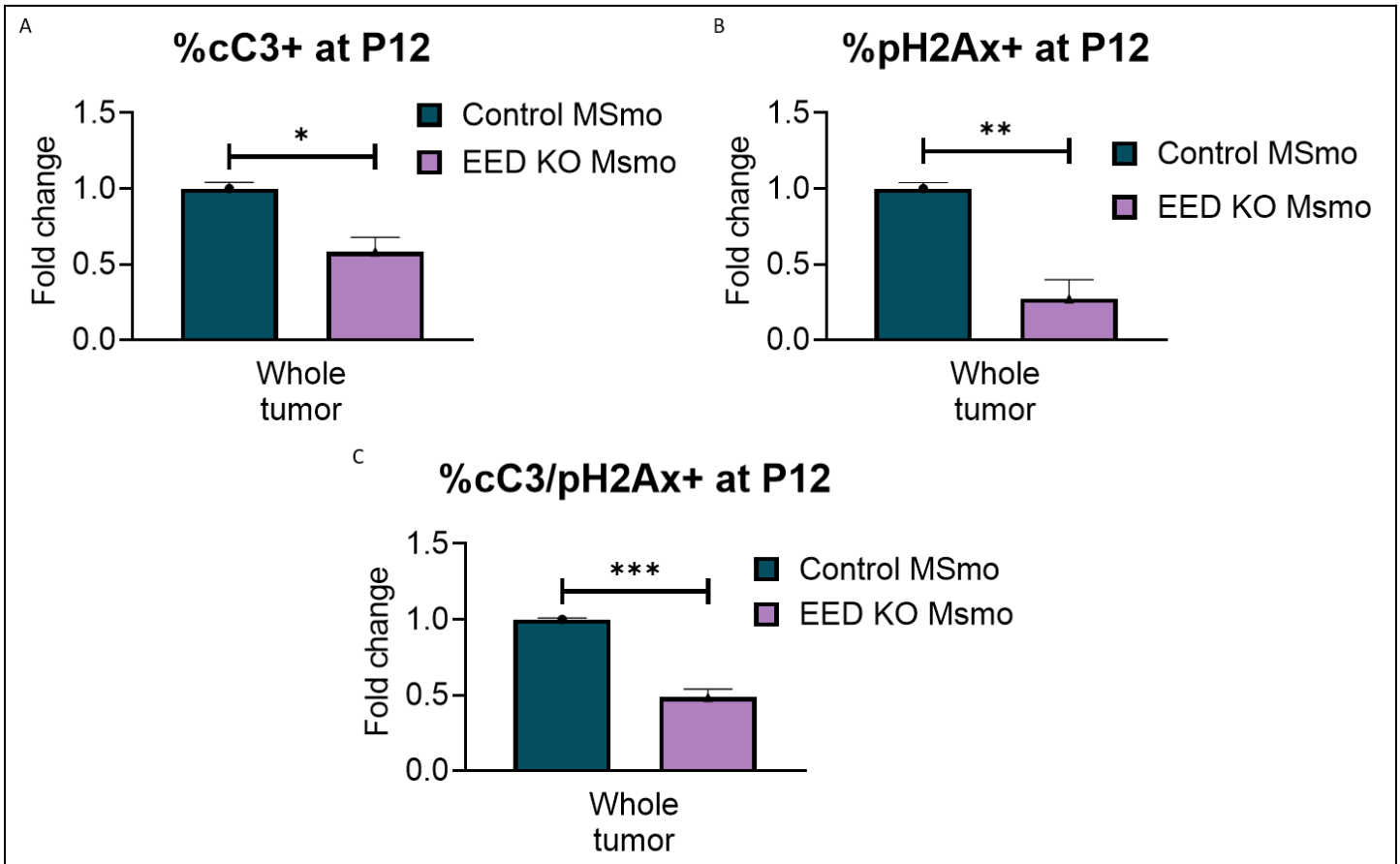

Figure 13: Immunohistochemistry (IHC) results for death markers. (A) cC3 is a marker for apoptosis (B) pH2Ax is a marker for DNA damage (C) cC3/pH2Ax is a co-expression marker for apoptosis and DNA damage. Statistical significance was calculated using unpaired two-tailed t-tests. "*" indicates that $p \leq 0.05$; "**" indicates that $p \leq 0.01$; "***" indicates that $p \leq 0.001$.

Eed cKO MSmo tumors showed significantly more myogenin expression compared to control MSmo tumors (**Figure 14A**). The increased expression of myogenin was not only seen across the whole tumor, but also in the hypercellular tumor-dense region. We did not, however, detect an increase in troponin (TNNT3; **Figure 14B**), as we previously saw in the Eed-deleted cerebellum.

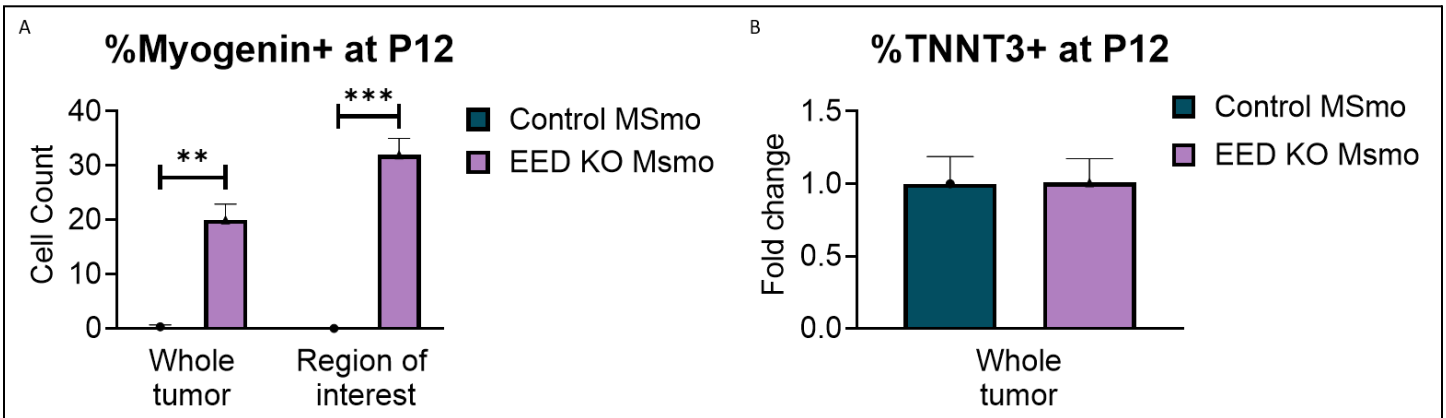

Figure 14: Immunohistochemistry (IHC) results for muscle proteins. (A) Myogenin is a protein found in muscles (B) TNNT3 is a marker for the muscle protein troponin. Statistical significance was calculated using unpaired two-tailed t-tests. "*" indicates that $p \leq 0.05$; "**" indicates that $p \leq 0.01$; "***" indicates that $p \leq 0.001$.

DISCUSSION

Both fluorescence-activated cell sorting (FACS) and immunohistochemistry (IHC) data showed a decreased proportion of proliferating cells in *Eed* cKO MSmo tumors compared to control MSmo tumors at P12, indicating that there are more cells exiting the cell cycle at that point in time when EED is not present. However, FACS studies showed that at P12, *Eed* cKO MSmo tumors have an increased proportion of proliferating cells in S phase; and that *Eed* cKO MSmo tumors at P12 have a greater proportion of proliferating cells in M phase compared to *Eed* cKO tumors at P18. Collectively, these data points lead to the conclusion that although there are more cells exiting the cell cycle at P12 in *Eed* cKO MSmo tumors, of the ones that remain, they are cycling faster than in control MSmo tumors.

By the time the mice reach P18, FACS data shows that some of these changes are compensated so that the cell cycle dynamics of the *Eed* cKO tumors are not as different from control MSmo tumors. There is a significant increase in the proportion of proliferating cells in *Eed* cKO tumors from P12 to P18 so that *Eed* cKO tumors no longer differ in that regard from control MSmo tumors. However, even at P18, there continues to be a greater proportion of proliferating cells in S phase, indicating that proliferating cells are still cycling faster in *Eed* cKO MSmo tumors than in control MSmo tumors. Thus, based on the cell cycle studies conducted here, *Eed* deletion slows tumor growth in early development, but the tumor later develops resistance, resulting in decreased survival.

Overall, at P12, through IHC data, *Eed*-deleted tumors showed reduced proliferation (decreased pRB), reduced neural differentiation (decreased NeuN), reduced apoptosis (decreased cC3), and aberrant muscle differentiation (Myog). While preliminary studies also showed decreased differentiation and proliferation in *Eed*-deleted CGNPs, an opposite phenotype was observed in regards to apoptosis. Additionally, *Eed* cKO MSmo tumors had equivalent amounts of p21 compared to MSmo tumors while *Eed*-deleted CGNPs had increased p21 expression. In cerebellar CGNPs, *Eed* deletion invokes increased expression of both myogenin and troponin (TNNT3); however, when deleting *Eed* in MSmo tumors, it only causes increased aberrant expression of myogenin, not troponin. The lack of increased troponin expression suggests that in tumors, unlike *Eed*-deleted cerebella, later stages of muscle differentiation were blocked. Since both proliferation and neural differentiation were reduced, muscle differentiation may have been an alternative fate for tumor cells exiting the cell cycle, and pRB studies in the MYOG+ population are needed to test the possibility.

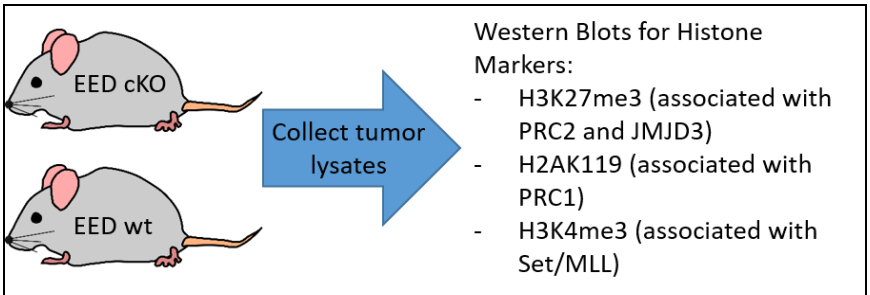

Figure 15: Future directions to determine the epigenetic complexes through which *Eed* deletion invokes the observed phenotypes.

Although the experiments presented here help better characterize the impacts of deleting EED in medulloblastoma tumors, a more thorough understanding of needs to be developed before EED or other members of the PRC2 can be implicated in molecular therapies. EED is predominantly found in PRC2 but also in PRC1, and these interact with other complexes like SET1/MLL and JMJD3 to regulate SHH-target gene expression. Thus, EED interacts with various epigenetic complexes through which *Eed* deletion can potentially invoke the observed phenotypes. As an extension of this project, one could better define exactly which complexes might contribute toward this phenotype by

measuring the levels of specific histone modifications. This would entail collecting tumor lysates and performing western blots for various histone markers such as H3K27me3 (associated with PRC2 and JMJD3), H2AK119 (associated with PRC1), and H3K4me3 (associated with SET1/MLL) (**Figure 15**). Identifying which changes in histone modifications correlate with *Eed* deletion will better elucidate what mechanisms and complexes, with which EED associates, are responsible for driving these phenotypes. By understanding how SHH signaling regulates target gene expression and the mechanisms of *Eed* deletion in medulloblastoma mouse models, researchers may be able to develop novel therapeutics for SHH-driven medulloblastoma.

REFERENCES

(1) Cheng, X.-S., Li, M.-S., Du, J., Jiang, Q.-Y., Wang, L., Yan, S.-Y., Yu, D.-M., and Deng, J.-B. (2011) Neuronal Apoptosis in the Developing Cerebellum. *Anat. Histol. Embryol. 40,* 21-27.

(2) Mochida, G. H., and Walsh, C. A. (2001) Molecular genetics of human microcephaly. *Curr. Opin. Neurol. 14,* 151-6.

(3) Chizhikov, V., and Millen, K. J. (2003) Development and malformations of the cerebellum in mic. *Mol. Genet. Metab. 80,* 54-65.

(4) Garcia, I., Crowther, A. J., Gama, V., Ryan Miller, C., Deshmukh, M., and Gershon, T. R. (2013) Bax deficiency prolongs cerebellar neurogenesis, accelerates medulloblastoma formation and paradoxically increases both malignancy and differentiation. *Oncogene 32,* 2304-2314.

(5) Vezina, G., Bayer, L., Packer, R. J., Gajjar, A., Rorke-Adams, L., Burger. P. C., Robertson, P. L., Lafond, D., Donahue, B. R., Maymont, M. H., Muraszko, K., Langston, J., and Sposto, R. (2006) Phase III Study of Craniospinal Radiation Therapy Followed by Adjuvant Chemotherapy for Newly Diagnosed Average-Risk Medulloblastoma. *Artic. J. Clin, Oncol. 24,* 4202-4208.

(6) Ramaswamy, V., and Taylor, M. D. (2017) JOURNAL OF CLINICAL ONCOLOGY Medulloblastoma: From Myth to Molecular. *J Clin Oncol 35*.

(7) Palmer, S. L., Reddick, W. E., and Gajjar, A. Understanding the Cognitive Impact on Children Who are Treated for Medulloblastoma.

(8) Mulher, R. K., Hancock, J., Fairclough, D., and Kun, L. (1992) Neuropsychological status of children treated for brain tumors: A critical review and integrative analysis. *Med. Pediatr. Oncol. 20,* 181-191.

(9) Crowther, A. J., Ocasio, J. K., Fang, F., Meidinger, J., Wu, J., Deal, A. M., Chang, S. X., Yuan, H., Schmid, R., Davis, I., and Gershon, T. R. (2016) Radiation Sensitivity in a Preclinical Mouse Model of Medulloblastoma Relies on the Function of the Intrinsic Apoptotic Pathway. *Cancer Res. 76,* 3211-23.

(10) Lewis, P. M., Gritli-Linde, A., Smeyne, R., Kottmann, A., and McMahon, A. P. (2004) Sonic hedgehog signaling is required for expansion of granule neuron precursors and patterning of the mouse cerebellum. *Dev. Biol. 270,* 393-410.

(11) Dey, J., Ditzler, S., Knoblaugh, S. E., Hatton, B. A., Schelter, J. M., Cleary, M. A., Mecham, B., Rorke-Adams, L. B., and Olson, J. M. (2012) A Distinct Smoothened Mutation Causes Severe Cerebellar Developmental Defects and Medulloblastoma in a Novel Transgenic Mouse Model. *Mol. Cell. Biol. 32,* 4104-4115.

(12) Shi, X., Zhang, Z., Zhan, X., Cao, M., Satoh, T., Akira, S., Shpargel, K., Magnuson, T., Li, Q., Wang, R., Wang, C., Ge, K., and Wu, J. (2014) ARTICLE An epigenetic switch induced by Shh signalling regulates gene activation during development and medulloblastoma growth.

(13) Scelfo, A., Piunti, A., and Pasini, D. (2015) The controversial role of the Polycomb group proteins in transcription and cancer: How much do we not understand Polycomb proteins? *FEBS J.*

(14) Crowther, A. J., Gama, V., Bevilacqua, A., Chang, S. X., Yuan, H., Deshmukh, M., and Gershon, T. R. (2013) Tonic Activation of Bax Primes Neural Progenitors for Rapid Apoptosis through a Mechanism Preserved in Medulloblastoma.

(15) Cao, Q., Wang, X., Zhao, M., Yang, R., Malik, R., Qiao, Y., Poliakov, A., Yocum, A. K., Li, Y., Chen, W., Cao, X., Jiang, X., Dahiya, A., Harris, C., Feng, F. Y., Kalantry, S., Qin, Z. S., Dhanasekaran, S. M., and Chinnaiyan, A. M. (2014) The central role of EED in the orchestration of polycomb group complexes. *Nat. Commun. 5*.

ACKNOWLEDGEMENTS

I would like to thank Abigail Cleveland and Dr. Timothy Gershon for allowing me to work as an undergraduate researcher in their lab and providing me with the training and support I needed to successfully complete a senior honors thesis. I would also like to thank Dr. Kelly Giovanello in the Department of Psychology and Neuroscience for providing me this opportunity and overseeing my progress for the past year. I would also like to acknowledge the assistance received from Hillary Heiling in conducting statistical analyses for this project. The FACS experiments were conducted in collaboration with the UNC Flow Cytometry Core Facility. This project was supported by funding from the *William W. and Ida W. Taylor Fellowship* administered by the Office for Undergraduate Research (OUR) and the *Tom and Elizabeth Long Excellence Fund for Honors* administered by Honors Carolina.